

Hyperspectral analysis of EO-1 Hyperion imagery: A case study in the geographical area of Greece

P. Stournara¹, M. Tsakiri-Strati², P. Patias²

1 Dr, M., 2 Professor

School of Rural and Surveying Engineering,

Department of Cadastre, Photogrammetry and Cartography,

Laboratory of Photogrammetry and Remote Sensing, AUTH

Abstract: The hyperspectral analysis was performed with a Hyperion image, which was captured in 2001 over the Greek area from the lake Kerkini north to the mountain Kissavos in Thessaly south. The analysis included the atmospheric correction of the image, the MNF (Minimum Noise Fraction) transformation, the PPI (Pixel Purity Index)/n-Dimensional visualization procedures as well as the SAM (Spectral Angle Mapper) classification. The final product of the analysis was thematic images of land use types. Hyperspectral data are imagery of very high spectral resolution. This characteristic allows the distinction between materials that generally may be very similar, but have some spectral characteristics that distinguish between them. This fact made the whole analysis even more interesting and important, as well as more challenging.

1. Introduction

The atmosphere affects solar radiation recorded by the satellite imaging system differently in the various wavelengths of the electromagnetic spectrum due to absorption and scattering. In ideal conditions, the solar radiation, which is captured by the satellite sensor, depends only on the radiation that comes from the study area. In reality, however, extra sunlight enters the field of view of the sensor introducing noise in the data. This additive effect of the atmospheric radiation due to absorption and scattering in the radiation recorded by the sensor on the image is called “atmospheric error” (Dermanis & Biagi, 2002; Jensen, 2005; Tsakiri-Strati, 2006; Stournara, 2007).

Hyperspectral Imagery (HSI) data, acquired using airborne or satellite systems, consist of many contiguous spectral bands. HIS data are of high spectral resolution because of their narrow bandwidth (10-15nm), contrary to multispectral data, the spectral resolution of which is significantly lower (1 μm = 100 nm). For this reason spectral information coming from HSI data is more accurate and detailed than spectral information coming from multispectral data (Figure 1). Because of this fact the atmospheric errors due to scattering and absorption are more evident in hyperspectral images than in multispectral ones. The atmospheric correction of

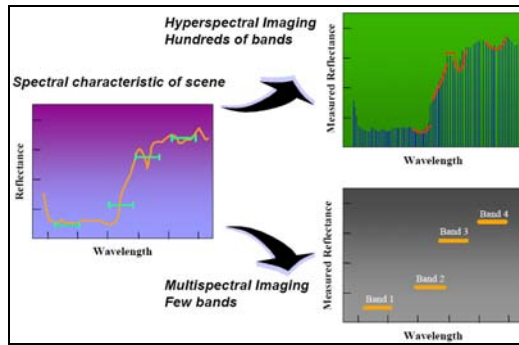


Figure 1. Comparison between multispectral and hyperspectral imaging (Pearlman et al., 2001).

them is necessary and more significant in the case of hyperspectral imagery (Tsakiri-Strati, 2006; Stournara, 2007). As is shown in Figure 1 (Pearlman et al., 2001) the spectral characteristic of scene (left) is not clear in multispectral imaging (right down) as in hyperspectral imaging (right up).

2. EO-1/Hyperion

The Hyperion sensor collects hyperspectral image data over the continuous spectrum from 356 to 2577 nm with a spatial resolution of 30 meters and a spectral resolution of 10nm. 198 of the collected bands are calibrated. The rest ones are uncalibrated and contain no information. Hyperion is carried on board EO-1 (Earth Observing-1) satellite, which was launched from Vandenberg Air Force Base on November 21, 2000 (Folkman et al., 2001; URL1).

Hyperion is a pushbroom instrument collecting data with a swath width of 7.7 km. Each scene covers a ground area of approximately 42 km or 185 km in the along-track direction. The system has two spectrometers: one visible/near infrared (VNIR) spectrometer (356-1058nm) and one short-wave infrared (SWIR) spectrometer (852-2577nm) (Folkman et al., 2001; URL1).

The Hyperion data are distributed by the USGS (U.S. Geological Survey). The Level 0 Hyperion data is the raw data, the Level 1R is only radiometrically corrected and the Level 1Gst Hyperion data is radiometrically corrected and systematically terrain-corrected (Folkman et al., 2001; URL1).

2.1. Hyperion imagery and study area

A Level 1R Hyperion scene was used in this study. The size of the Hyperion image was 7.7×185km. The study area extends from the lake Kerkini in northern Greece to the area of mountain Kissavos in Thessaly. It includes the urban area of Thessaloniki.

3. Analysis Methodology

The methodology applied in the analysis of the Hyperion image consisted of the following steps:

- i) Atmospheric correction using FLAASH (Fast Line-of-sight Atmospheric Analysis of Spectral Hypercubes).
- ii) Spectral compression, dimensionality reduction, noise reduction using the Minimum Noise Fraction (MNF) transformation.
- iii) Determination and extraction of the endmembers, utilizing the Pixel Purity Index (PPI) and n-Dimensional Visualizer.
- iv) Identification of endmember spectra using visual comparison with known library spectra.
- v) Classification with the use of Spectral Angle Mapper (SAM) algorithm.

Through this approach no “a priori” knowledge or ground observations are required in order to extract spectral information from hyperspectral data. This methodology was applied in the ENVI 4.3 software.

4. Atmospheric Correction

The goal of the atmospheric correction is to reduce or remove completely, if possible, the absorption and scattering effects of the Earth’s atmosphere in order to allow conversion of the image data from radiance recorded at the sensor to surface reflectance (Stournara, 2007). In this study the algorithm of FLAASH was utilized to remove the atmospheric errors. It creates an image of retrieved surface reflectance.

FLAASH belongs to the atmospheric modeling approaches that attempt to quantify the exact atmospheric composition at the time of data acquisition and then calculate the probable effects of the atmosphere. In order to achieve this, various parameters are required, such as time and date of image acquisition, aerosol model (eg. rural, urban, maritime) according to land cover type, sensor information etc. It was developed by Spectral Sciences, Inc. in collaboration with the U.S. Air Force Research Laboratory (AFRL) and the Spectral Information Technology Application Center (SITAC) personnel in U.S.A. FLAASH uses MODTRAN (MODerate resolution TRANsmittance code) which is one of the atmospheric transmission codes. MODTRAN calculates the multiple scattering of the solar radiation at the time of data acquisition (Envi User’s Guide, 2006; Erdas User’s Guide).

4.1. Wavelength Recalibration

An accurate wavelength calibration is critical for atmospherically correcting hyperspectral data. Even slight errors in the locations of band center wavelengths can

introduce significant errors and reduce the overall accuracy of the modeled surface reflectance results (Envi User’s Guide, 2006). To minimize such errors, FLAASH supports wavelength recalibration.

4.2. Spectral Polishing

Spectral polishing reduces spectral artifacts in hyperspectral data using only the data itself. It uses Legendre polynomial fitting for smoothing. A running average over n adjacent channels (where n is defined as the polishing width) is performed. A value of 9 is recommended for typical 10 nm-resolution hyperspectral sensors, (Envi User’s Guide, 2006).

5. MNF (Minimum Noise Fraction) Transformation

MNF transformation is used to reduce the dimensionality of hyperspectral data and minimize the noise in the hyperspectral image. The MNF is used to determine the inherent dimensionality of the hyperspectral data, to identify and separate noise from useful information in the hyperspectral data and to reduce simultaneously the computation requirements of further hyperspectral processing (Jensen, 2005). The MNF transformation is a linear transformation related to the principal components- the order of the MNF data is according to the signal to noise ratio, (Kruse, 2003).

5.1. Inverse MNF Transformation

The inverse MNF transformation is used to transform the MNF bands back to their original data space i.e. to the original number of bands (Envi User’s Guide, 2006). It was applied to a selected set of MNF bands, which contained the valuable information of the Hyperion scene, in order to reduce the noise and remove the bad columns of the image. Generally, bad columns in the image datasets come from detectors of the satellite system that didn’t function well during the imagery collecting

Table 1. Bad columns and corresponding bands of the Hyperion image data.

Band	Bad Column	Band	Bad Column
8	6, 68, 114, 238	99	91
9	6, 68, 114, 222	116	137
10-11	6, 114, 199	119	239
12-20	114	190	112
27-28	47, 114	191-192	245
55	13, 17, 20	200-201	7
94	92	203	114

(Tsakiri-Strati, 2004). Table 1 lists the detected bad columns in the Hyperion image. Bad columns can be removed with the use of the inverse MNF transformation.

6. PPI (Pixel Purity Index)/n-Dimensional Visualizer

For the determination and extraction of the spectral profiles of the land use types of the Hyperion scene the PPI and n-Dimensional Visualization processing were utilized in ENVI 4.3 software. In this processing only the MNF bands with the useful information are used as input.

Endmembers are unique materials in the satellite image, which are spectrally pure. The PPI processing is designed to locate the most spectrally pure pixels of the satellite image, but typically these pixels, when found, are mixing endmembers (Envi User's Guide, 2006), so further processing is needed.

Spectra can be thought of as points in an n-dimensional. In this n-dimensional space n is the number of bands. The PPI is computed by repeatedly projecting n-dimensional scatterplots onto a random unit vector. In each iterative projection the extreme pixels are marked and counted. Then, a PPI image is created in which the digital number of each pixel is the number of times that pixel was counted as extreme. Finally a threshold is interactively selected using the histogram of the PPI image in order to choose only the purest pixels, which will be used in n-Dimensional Visualization (Kruse, 2003; Envi User's Guide, 2006).

"n-D Visualizer" is a technique of visualizing these points and determining of the spectral profiles of the categories (classes) of the Hyperion image. Spectra of the endmembers are used to extract the spectral profile of each category (class) of the Hyperion image. N is the number of spectral bands used to visualize these data. The PPI image is utilized to select only the purest pixels for visualization.

In this visualization (n-dimensional scatterplot) spectra act as points, where n is the number of bands. Considering a single pixel, the coordinates of the points in n -space consist of " n " values and constitute the spectral reflectance values in each hyperspectral band. The distribution of these points in n -space can be used to estimate the spectral endmembers of the image and after that their pure spectral profiles. To explain the procedure more thoroughly: If two endmembers mix, the mixed pixels will fall in a line in the histogram, while the pure endmembers will fall at the two ends of the mixing line. If three endmembers mix, then the mixed pixels will fall inside a triangle etc. After the proper pure pixels have been selected, mean spectra are extracted as spectral profiles of images' classes, which will be then used in the SAM classification (Kruse, 2003; Envi User's Guide, 2006).

7. SAM (Spectral Angle Mapper) Classification

The Spectral Angle Mapper method is utilized for comparing automatically image spectra to individual spectra (Kruse, 2003). Individual spectra used in this study came from the PPI/n-D Visualization processing of the Hyperion image.

The SAM algorithm determines the similarity between two spectra based on the calculation of the “spectral angle” between them. It treats them as vectors in a space with dimensionality equal to the number of bands. The method is insensitive to illumination. This is due to the fact that it uses only the vector direction of the spectra and not their vector length. The SAM classification result is a color-coded image, which shows the best SAM match at each pixel (Kruse, 2003). It was applied on the atmospherically corrected image.

The SAM classification was also tested to MNF data in combination with the inverse MNF transformation. Classification was applied to the Hyperion image after the removal of noise (only the first MNF bands with the useful information were kept). This was done for classification improvement.

8. Results

Results from the hyperspectral analysis of the Hyperion image are presented below.

8.1. Atmospheric correction results

Hyperion image includes regions of different land cover. Therefore Hyperion image was subset into 4 parts, which were atmospherically corrected separately, according to their land cover type (i.e. rural aerosol model was utilized for rural areas, maritime model for sea and urban model for urban area).

Due to wavelength recalibration there was a shift of band center wavelengths by 1.32nm to 1.62nm in the first 70 bands (VNIR spectral region) and by -13.54nm to -16.71nm in the next 71-242 bands (SWIR spectral region). In Figure 2, results from atmospheric correction with and without wavelength recalibration are shown. The change in vegetation spectral profile between the two cases can be noticed.

Atmospheric correction was applied to the Hyperion image with and without spectral polishing. Spectral artifacts are reduced with the use of spectral polishing. Results are shown in Figure 3. The arrows point out this reduction. In Figure 3c₁-c₃ emphasis is given to vegetation profiles in the spectral region of 650-850nm, the chlorophyll edge region. Artifact reduction is pointed out with a circle.

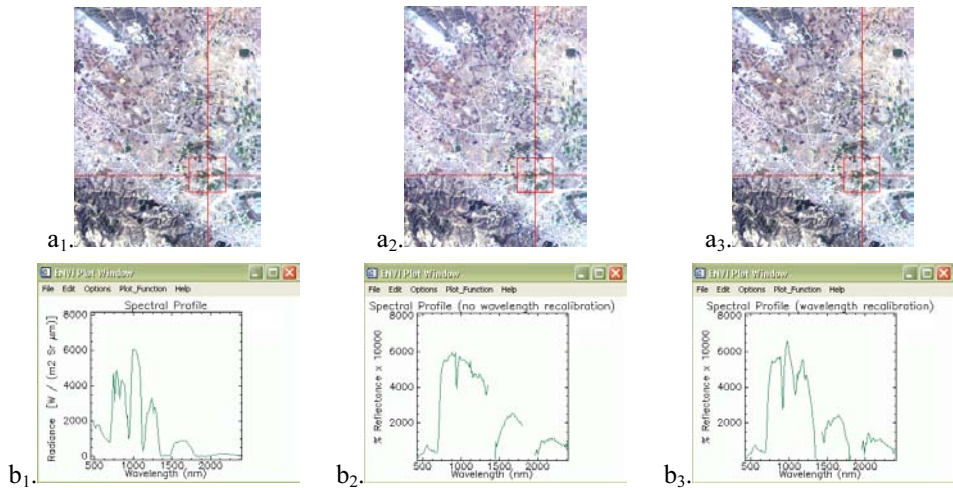


Figure 2. Part of the Hyperion scene, a_1 : radiance, a_2 : reflectance without wavelength recalibration, a_3 : reflectance with wavelength recalibration, b_1 - b_3 : vegetation spectral profile of the center pixel in the red box of a_1 - a_3 .

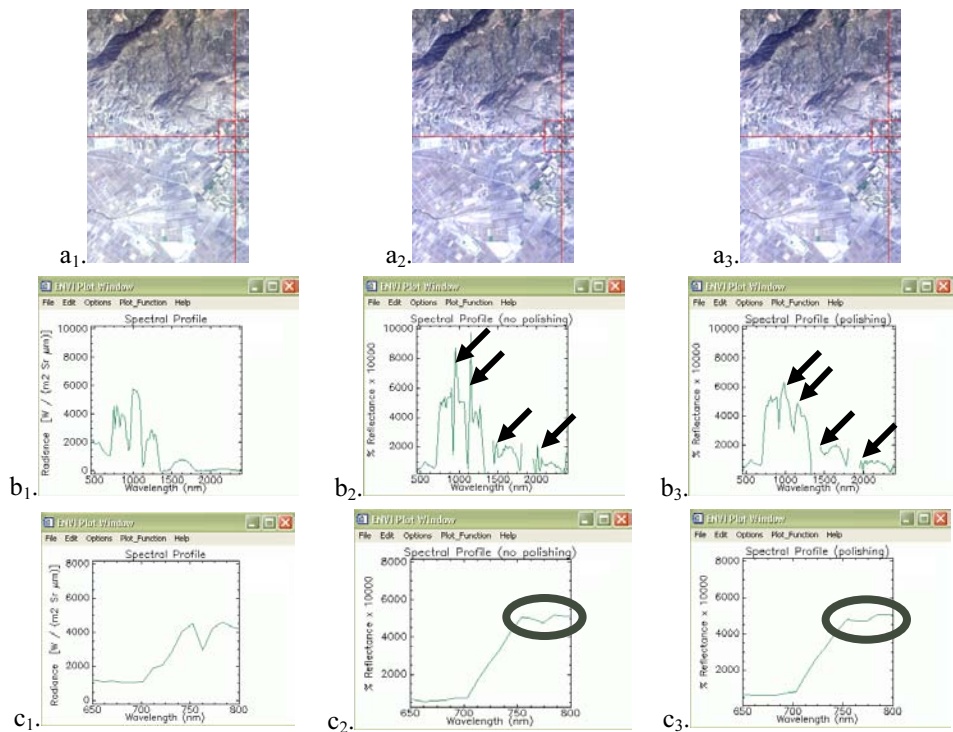


Figure 3. Part of the Hyperion scene, a_1 : radiance, a_2 : spectral unpolished reflectance, a_3 : spectral polished reflectance, b_1 - b_3 : Vegetation spectral profile of the center pixel in the red box of a_1 - a_3 , c_1 - c_3 : the chlorophyll edge region (650-850nm) of the spectral profile shown in b_1 - b_3 .

8.2. MNF results/Inverse MNF results

The MNF transformation was applied to the 3 atmospherically corrected parts of the Hyperion image with rural (agricultural, mountainous, semi-mountainous) and urban areas in order to separate the useful information of the image from noise. After the MNF, the useful information was accumulated in the first bands. Results from the MNF bands are shown in Figures 4-6.

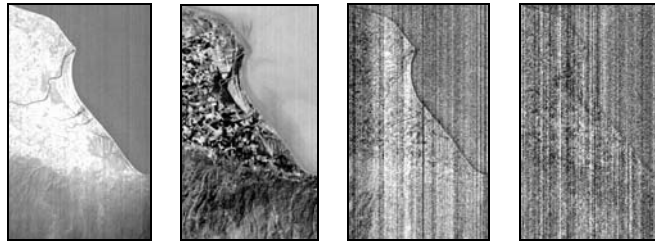


Figure 4. MNF bands 1, 5, 21 and 40 for the mountainous region of the Hyperion scene. From the 1st MNF band to the 40th MNF band the information of the band is reduced.

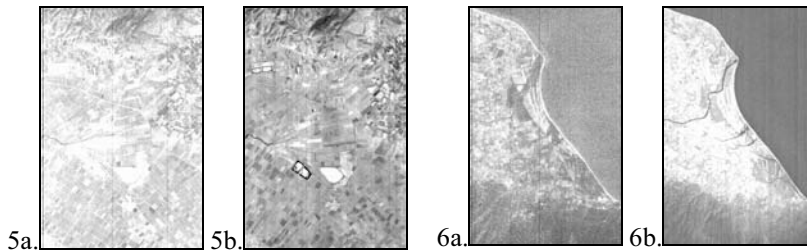


Figure 5. Part of the Hyperion scene, a: before the MNF transformation (10th band of the atmospherically corrected Hyperion scene -the first 7 bands contain no information), b: after the MNF transformation (3rd band).

Figure 6. Part of the Hyperion scene, a: before the MNF transformation (8th band of the atmospherically corrected Hyperion scene -the first 7 bands contain no information), b: after the MNF transformation (1st band).

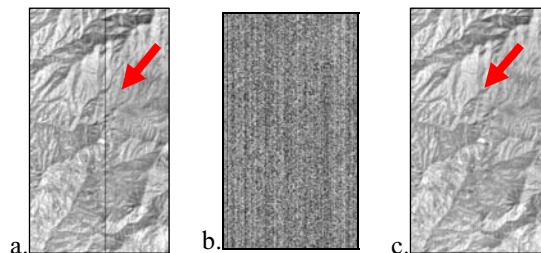


Figure 7. Part of the Hyperion scene, a) before the MNF transformation, b) after the MNF and, c) after the inverse MNF, (116th band). The bad column pointed out with the arrow in a, is not present in c.

The inverse MNF was applied to the Hyperion part with semi-mountainous and agricultural areas. In this way the bad column in Figure 7a has been removed in 7c.

8.3. PPI/n-Dimensional Visualizer results

Endmember and spectral profile extraction was applied separately for the 3 parts of the Hyperion image with rural (agricultural, mountainous, semi-mountainous) and urban areas. Extracted spectral profiles were representative of the Hyperion land cover types, i.e. lake, vegetation, buildings, bare land (Figures 8a₁ and 9a₁).

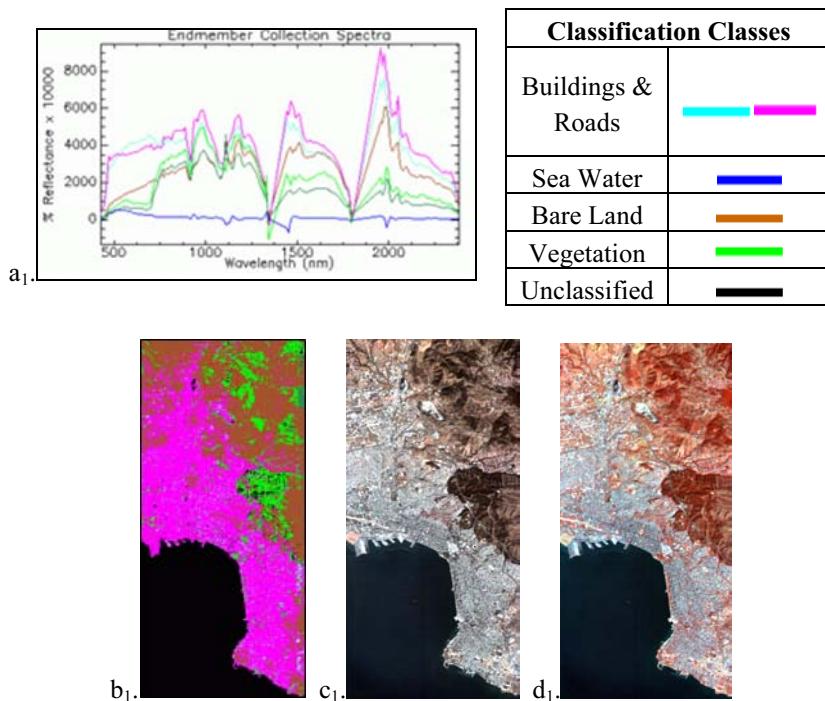


Figure 8. a₁: Spectral profiles, which were determined through the hyperspectral analysis for the urban part of the Hyperion image and were used in the SAM classification, b₁: The classified image, c₁: The urban study area in the atmospherically corrected Hyperion image (RGB=27 (red region, typical average wavelength of this band is 620.15nm)/17 (green region, typical average wavelength of this band is 518.39nm)/11 (blue region, typical average wavelength of this band is 457.34nm)), d₁: The urban study area in the atmospherically corrected satellite image (RGB=45 (near infrared region, typical average wavelength of this band is 803.30nm)/21 (green region, typical average wavelength of this band is 559.09nm)/12 (blue region, typical average wavelength of this band is 467.52nm)). In d₁ since the 45th infrared band is used in the RGB combination, vegetation is depicted with red colors in the image.

8.4. SAM classification results and Discussion

The SAM classification was applied to the urban part and the northern rural part of the Hyperion image (from the lake Kerkini until Thessaloniki). The spectral profiles of the classes were determined through the hyperspectral analysis described in paragraph 6 separately for each of the two parts. They were used as known spectra in each classification. The angle used in the SAM classification was 0.30 radians. The results are presented in Figures 8 and 9.

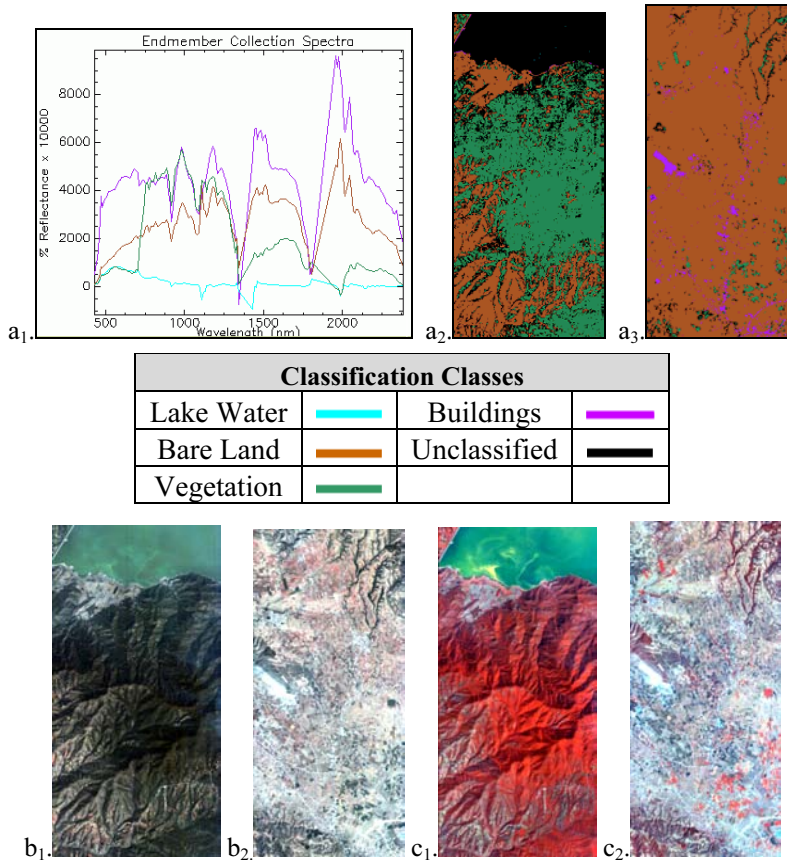






Figure 9. *a₁*: Spectral profiles of the classes of the Hyperion part with rural areas. They were determined through the hyperspectral analysis and were used in the SAM classification, *a₂-a₃*: The classified image, *b₁-b₂*: The same study area in the atmospherically corrected Hyperion image (RGB=27/17/11), *c₁-c₂*: The same area in the atmospherically corrected satellite image (RGB=45/21/12). In *c₁-c₂* since the 45th infrared band is used in the RGB combination, vegetation is depicted with red colors.

In Figure 8b₁, the thematic image is the result of the SAM classification. The urban area is very well mapped in the classified image, as it can be deduced from a visual comparison with the atmospherically corrected image (8c₁-8d₁). The urban sprawl north(west) is also very well mapped. In 8d₁, vegetation is shown with red color due to participation of the InfraRed (IR) band in the RGB combination (RGB=45/21/12). This explains the presence of vegetation class in 8b₁, although it is not evident in 8c₁.

The thematic image created from the SAM classification (Figure 9a₂-9a₃) depicts very well the land use classes of the Hyperion image, as can be seen when comparing the thematic image with the atmospherically corrected image in 9b₁-9b₂ (RGB=27/17/11) and 9c₁-9c₂ (RGB=45/21/12). In 9c₁-9c₂ vegetated areas are colored red, because of the participation of the IR band in the RGB combination. Bare land and vegetation are very well mapped, as well as some buildings in the rural area (9a₃, 9b₂, 9c₂).

Subsequently, the SAM classification was applied with the use of the inverse MNF transformation, after the removal of noise. This was done for the northern rural part of the image. Results are presented in Figure 10. As it can be seen the classification accuracy was improved. Both the overall accuracy and the K coefficient were better in the classification utilizing the inverse MNF (Table 2). This improvement can be noticed visually, especially in the lake area (Figure 10b). K coefficient ranges from 0 to 1. If it is equal to 1, then the classification is perfect. % Overall accuracy assesses the total classification accuracy.

Table 2. Classification Accuracy.		
SAM Classification	%Overall Accuracy	K coefficient
With inverse MNF	86.3485	0.8063
Without inverse MNF	82.4638	0.7502

Classification Classes	
Lake Water	
Bare Land	
Vegetation	
Unclassified	

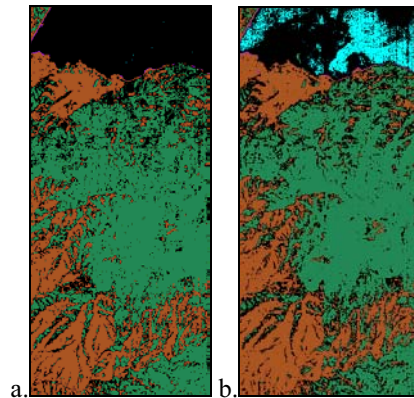


Figure 10. The SAM classification was applied to the atmospherically corrected image with or without MNF. Part of the classified image (Hyperion part with rural areas), a: without MNF and b: with MNF. Table 2 shows SAM classification accuracies for this study.

9. Conclusions

In this study the FLAASH algorithm was utilized for the atmospheric correction of the Hyperion image. Spectral polishing and wavelength recalibration improved the atmospheric correction results, as was evident from the spectral profiles. The PPI and n-D Visualization process were successful in extracting the spectral profiles of the classes. The SAM classification results show it clearly. Moreover, the vegetation spectral profiles extracted (Figures 8a₁ and 9a₁) are similar to the well-known vegetation spectral profile.

The MNF transformation applied helped in the reduction of the computational requirements and in noise removal. The use of the inverse MNF, after the removal of the MNF bands which included mainly noise, enabled the improvement of the SAM classification results.

The hyperspectral analysis followed created thematic images, in which land use types were very well mapped. This procedure can be utilized extensively in the production of thematic maps with considerable accuracy. Moreover, it could be applied to hyperspectral data, possibly of other hyperspectral sensors with greater spatial resolution, in order to extract information between similar classes.

References

- Dermanis, A. and Biagi, L., 2002. *Topics on remote sensing*. CEA Editions, Milano, 288pp.
- ENVI User's Guide, The ENvironment for Visualizing Images, 2006.
- ERDAS User's Guide, 2005.
- Folkman, M.A., Pearlman, J., Liao, L.B. and Jarecke, P.J., 2001. *EO-1/Hyperion hyperspectral imager design, development, characterization, and calibration*. Proc. SPIE, 4151: 40-51
- Jensen, J.R., 2005. *Introductory Digital Image Processing: A Remote Sensing Perspective*. Pearson Education, 3rd ed., 526 pp.
- Kruse, F.A., 2003. *Preliminary results-hyperspectral mapping of coral reef systems using EO-1 Hyperion, Buck island, U.S. Virgin Islands*. 12th JPL Airborne Geoscience Workshop, 2003, Pasadena, California.
- Pearlman, J., Segal, C., Clancy, P., Nelson, N., Jarecke, P., Ono, M., Beiso, D., Liao, L., Yokohama, K., Carman, S., Browne, B., Ong, L. and Ungar, S., 2001. *The EO-1 Hyperion Imaging Spectrometer*. IEEE Aerospace Conference, 11 pp.
- Shaw, G.A. and Burke, H., 2003. *Spectral Imaging for Remote Sensing*. Lincoln Laboratory Journal, Volume 14 (1).
- Stournara, P., 2007. *Evaluation of atmospheric correction techniques of hyperspectral Hyperion images*. MSc Dissertation, AUTH University, pp.226.

Tsakiri-Strati, M., 2006. *Hyperspectral Remote Sensing, University Lectures for post-graduate students.* (in Greek). AUTH, 180 pp.

Tsakiri-Strati, M, 2004. *Remote Sensing, University Tutorials for undergraduate students.* (in Greek), AUTH.

URLS

URL1-<http://eo1.usgs.gov/>